Machine-learned interatomic potential models for practical applications

Tim Mueller
Johns Hopkins University

Funded by the Toyota Motor Corporation and the Office of Naval Research

Contributors

Chuhong Wang

Adarsh Balasubramanian

Alberto Hernandez

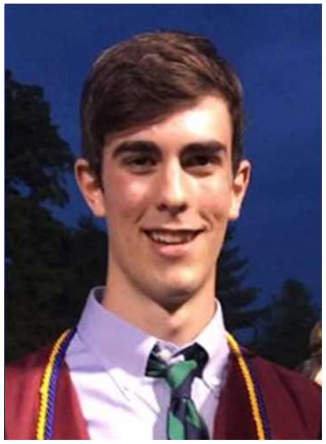

Simon Mason

Machine-learned interatomic potentials

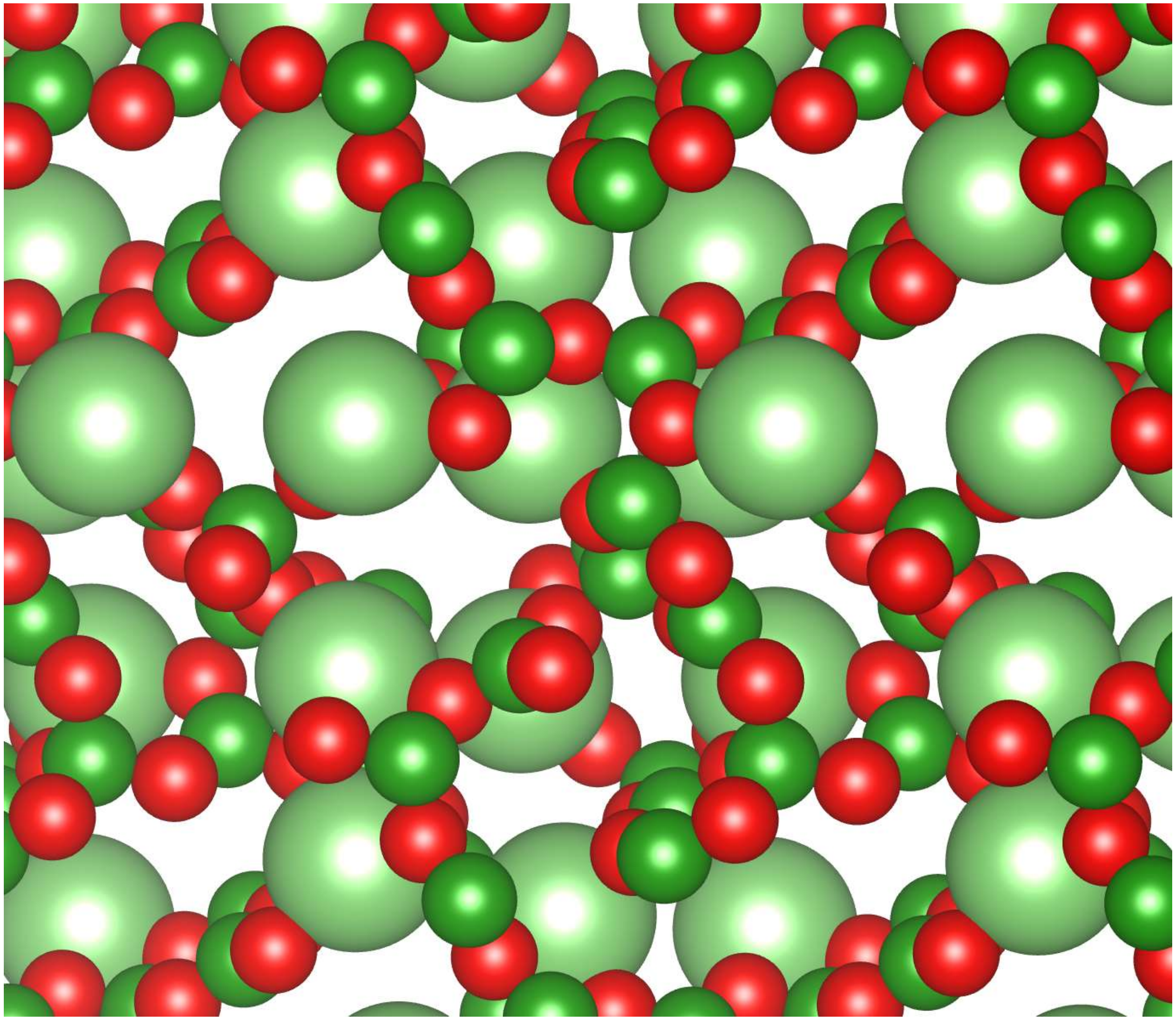

Machine-learned interatomic potentials

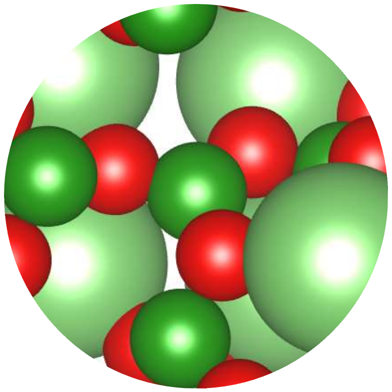

Moment tensor potentials

The energy is a polynomial of inner products of vectors between atoms and the vector lengths.

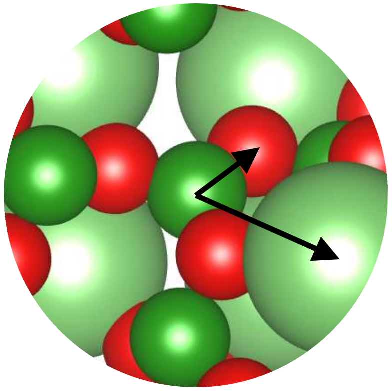

A. V. Shapeev, Multiscale Model. Simul., 14(3), 1153–1173.

Moment tensor potentials

The energy is a polynomial of inner products of vectors between atoms and the vector lengths.

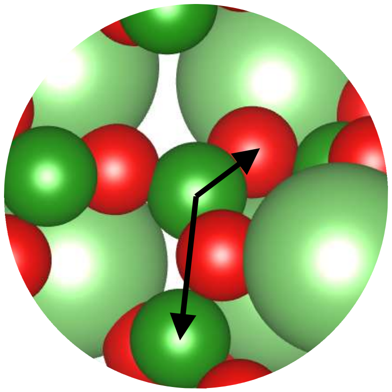

A. V. Shapeev, Multiscale Model. Simul., 14(3), 1153–1173.

Moment tensor potentials

The energy is a polynomial of inner products of vectors between atoms and the vector lengths.

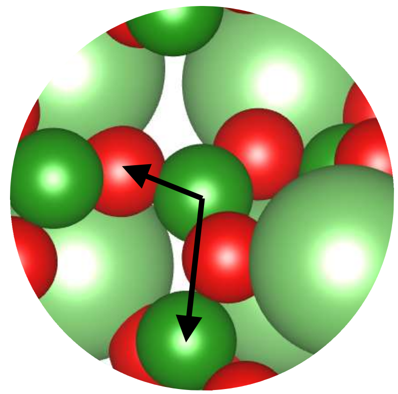

A. V. Shapeev, Multiscale Model. Simul., 14(3), 1153–1173.

Moment tensor potentials

The energy is a polynomial of inner products of vectors between atoms and the vector lengths.

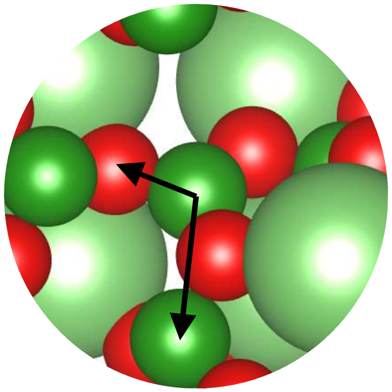

They demonstrate excellent balance between speed and interpolative predictive accuracy.

Y. Zuo et al., The Journal of Physical Chemistry A 124, 4, 731–745 (2020)

Lithium-ion batteries

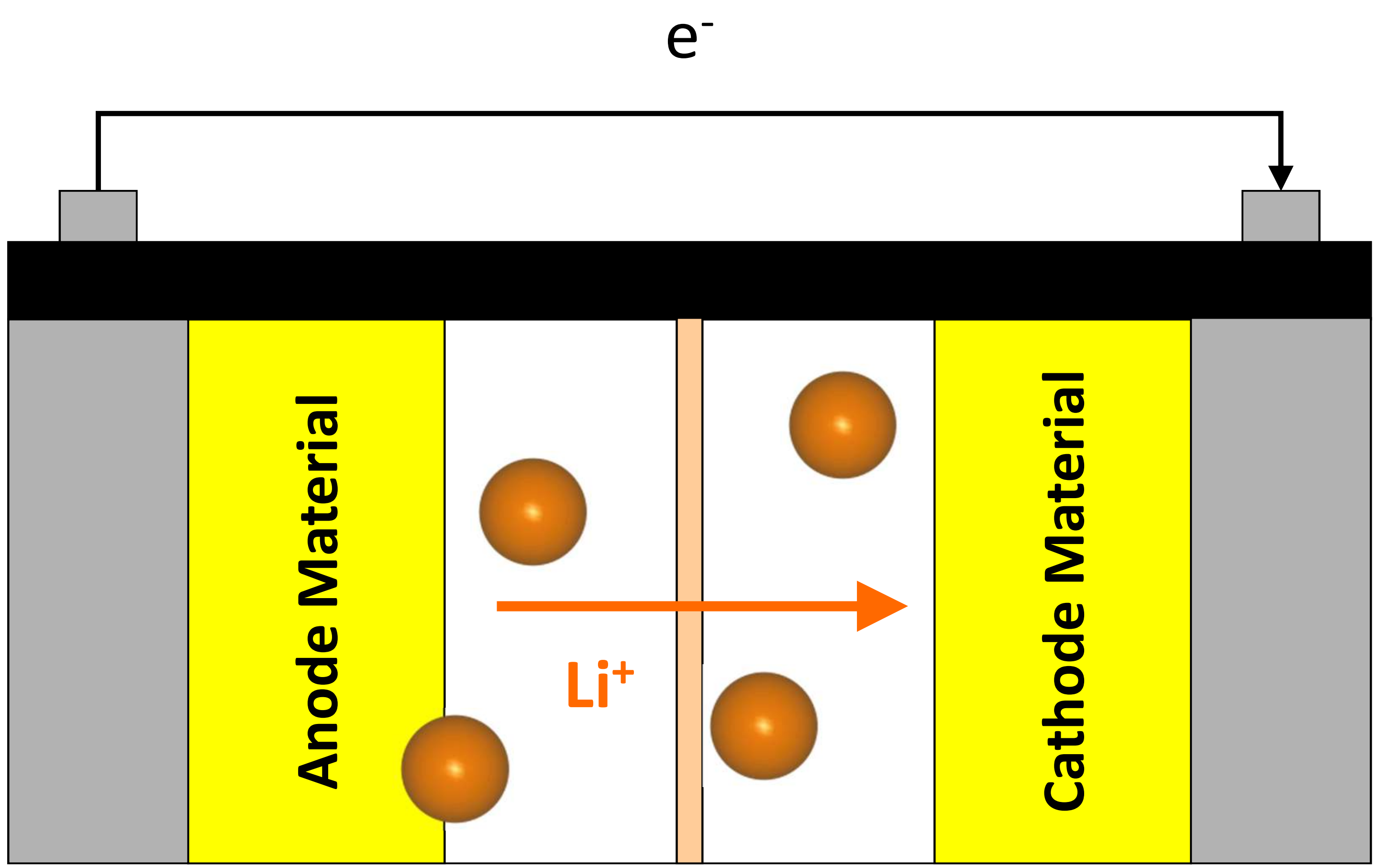

Lithium-ion batteries

JOHNS HOPKINS
WHITING SCHOOL
of ENGINEERING

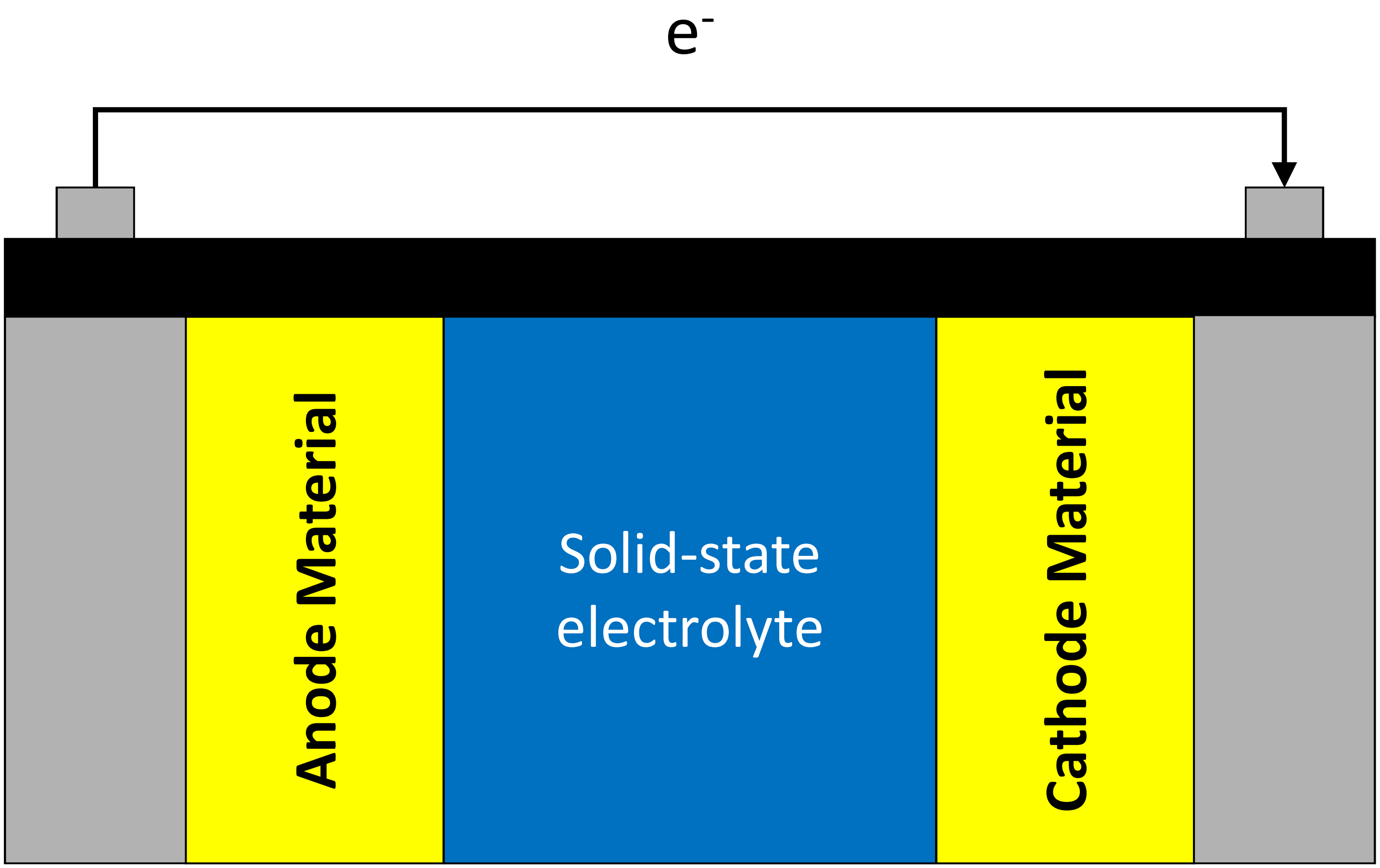

Lithium-ion batteries

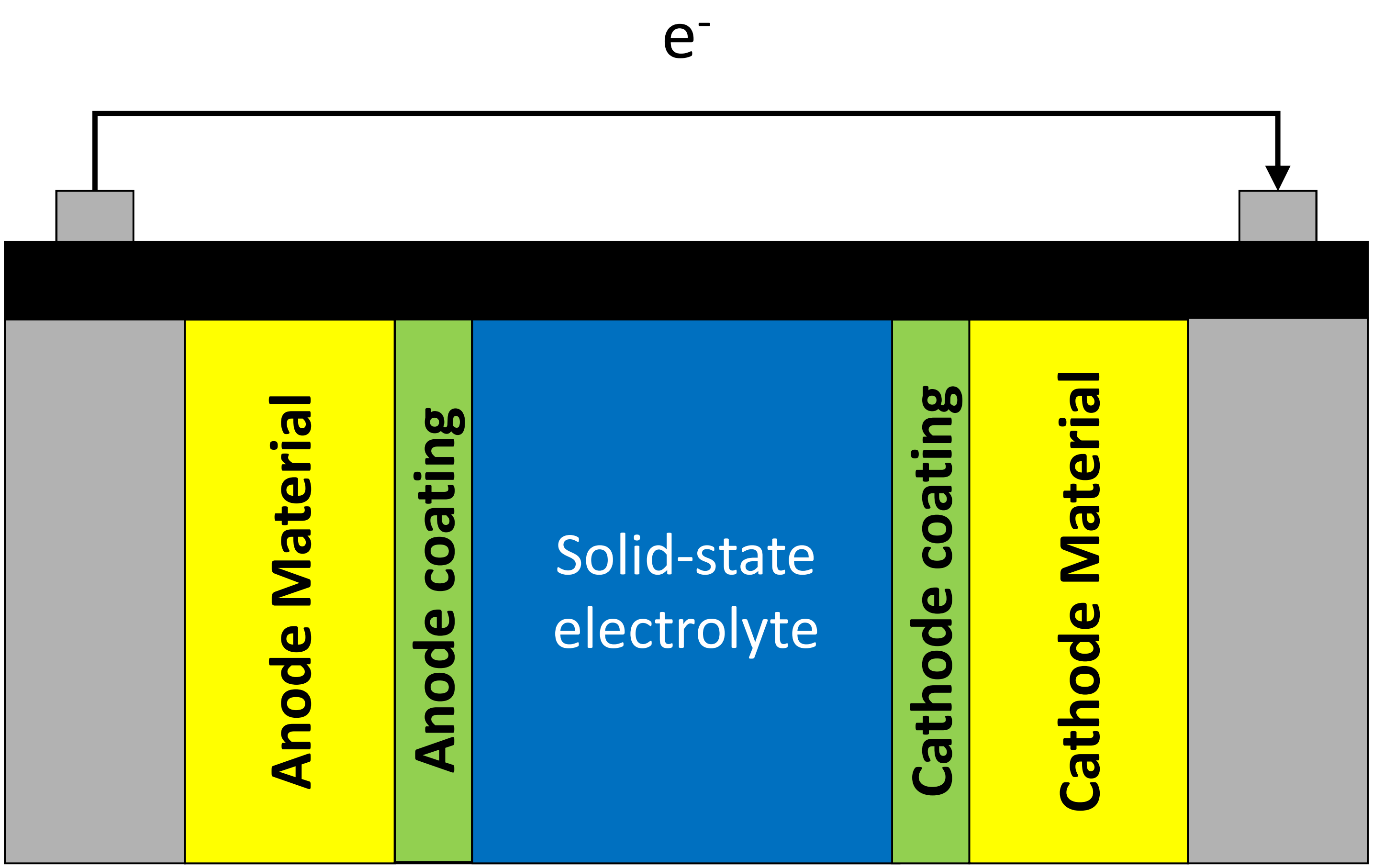

Lithium-ion batteries

In the anode and cathode, lithium ions typically diffuse by hopping into vacant sites.

The activation energy can be calculated using the nudged elastic band method.

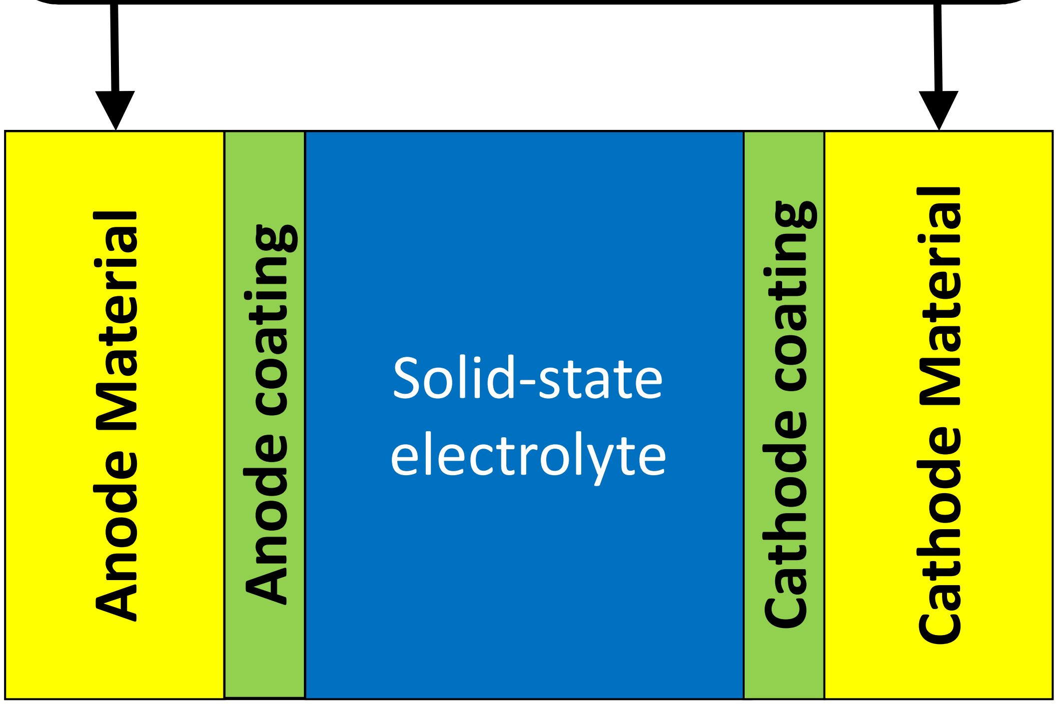

Lithium-ion batteries

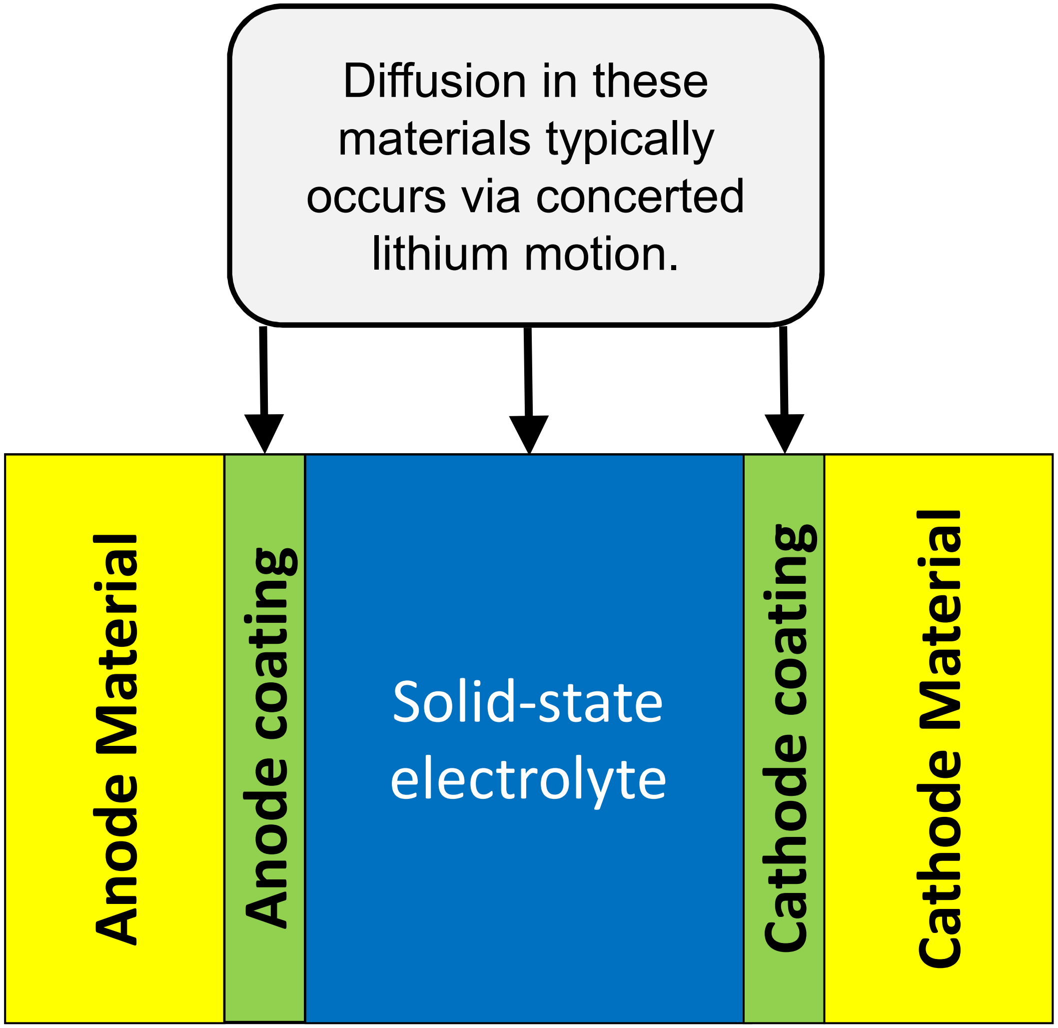

Concerted lithium-ion diffusion

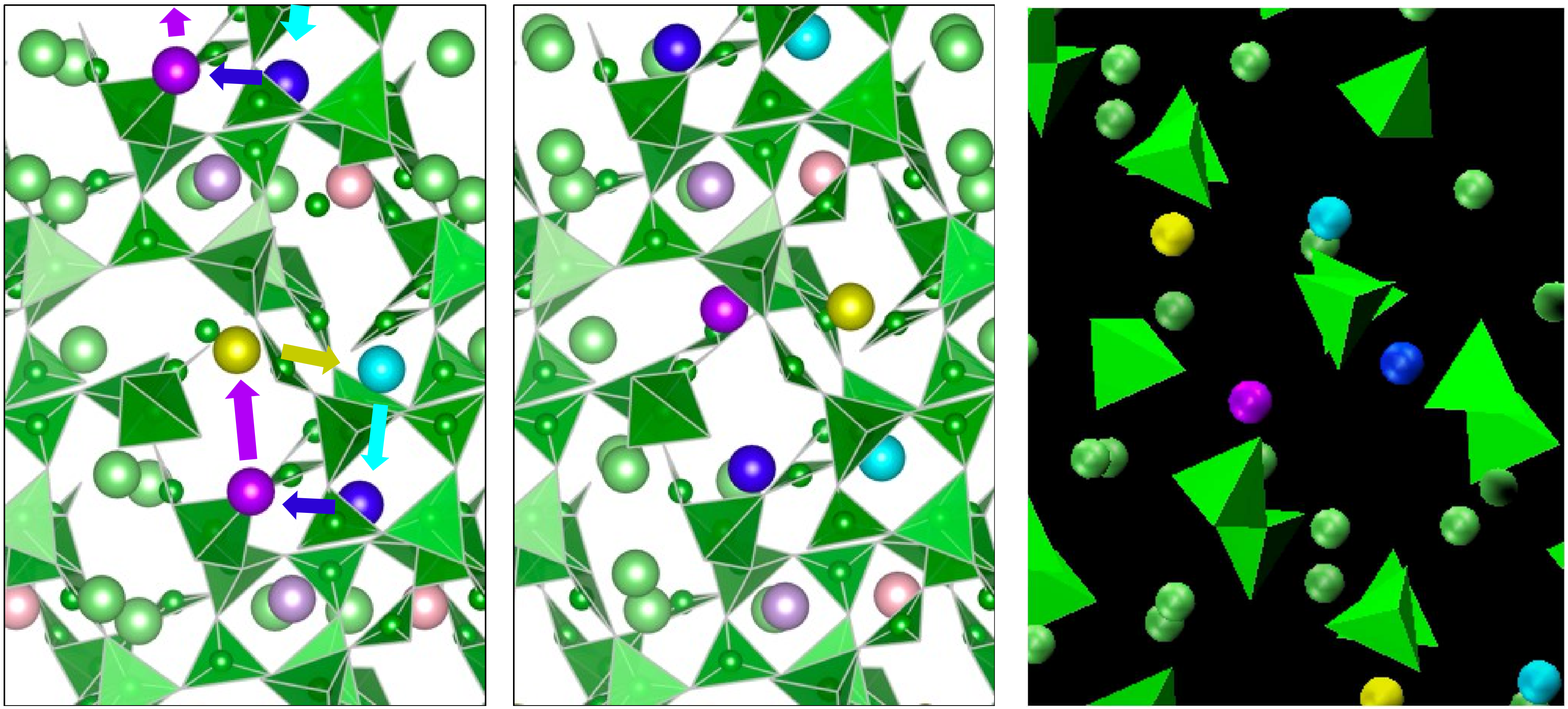

C. Wang, K. Aoyagi, P. Wisesa, and T. Mueller, Chemistry of Materials **32**, 9, 3741–3752 (2020)

Lithium-ion batteries

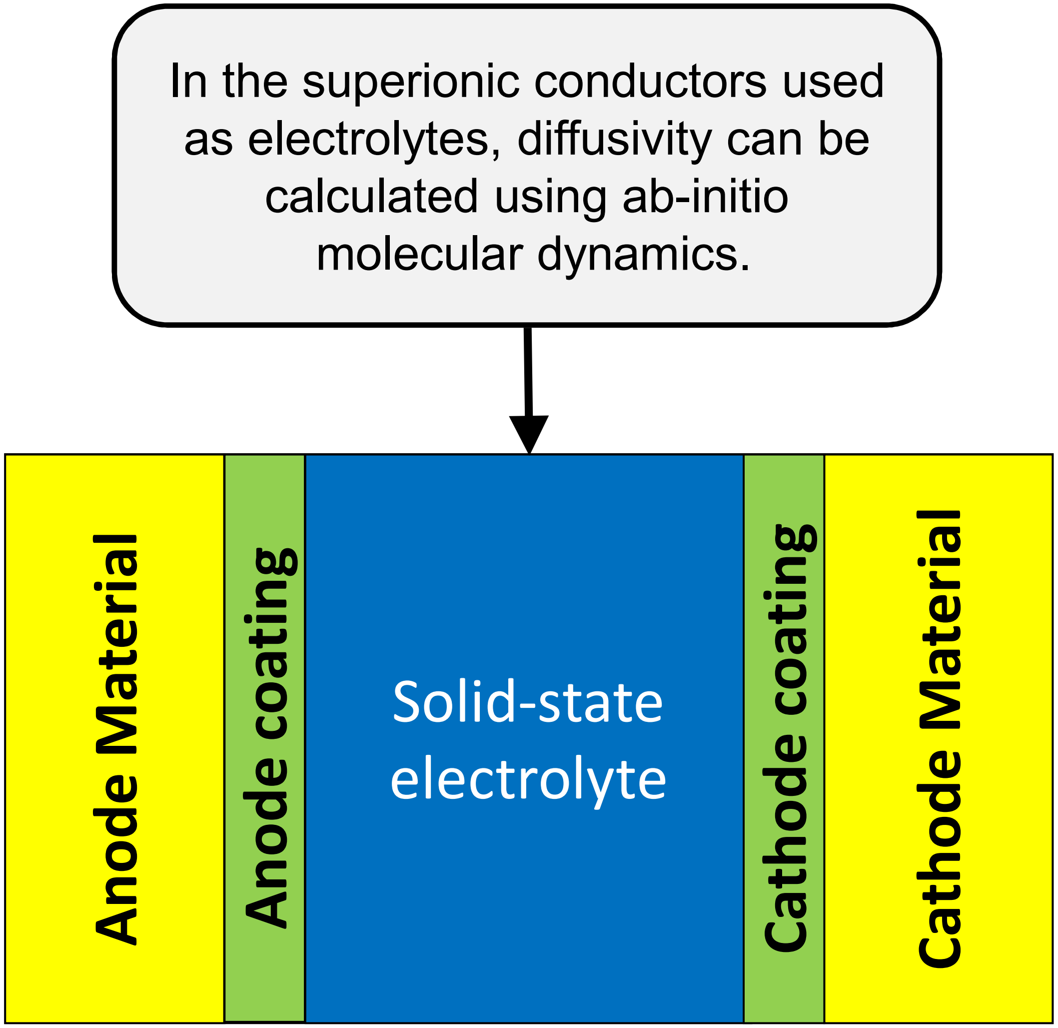

Lithium-ion batteries

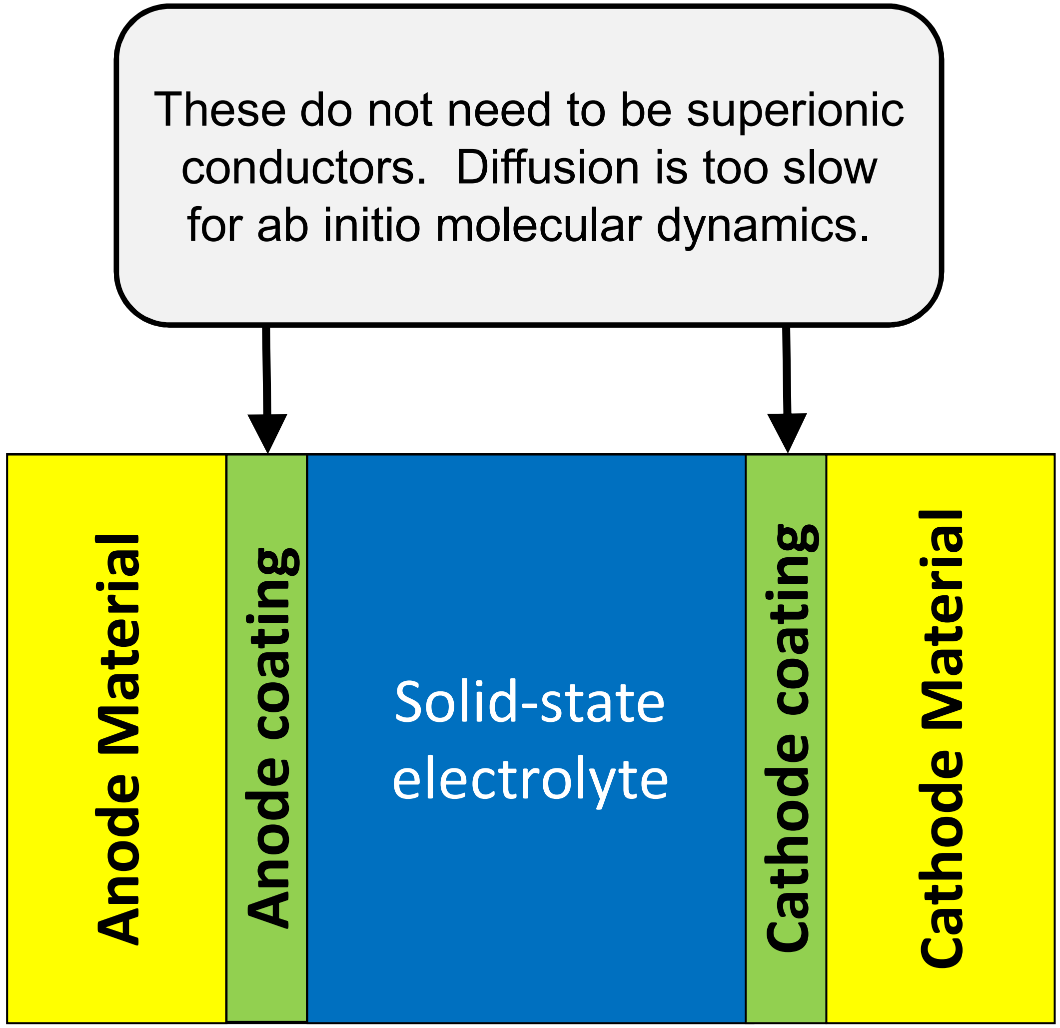

Ensuring high accuracy

Moment tensor potentials can be highly accurate for local configurations similar to ones used to train them.

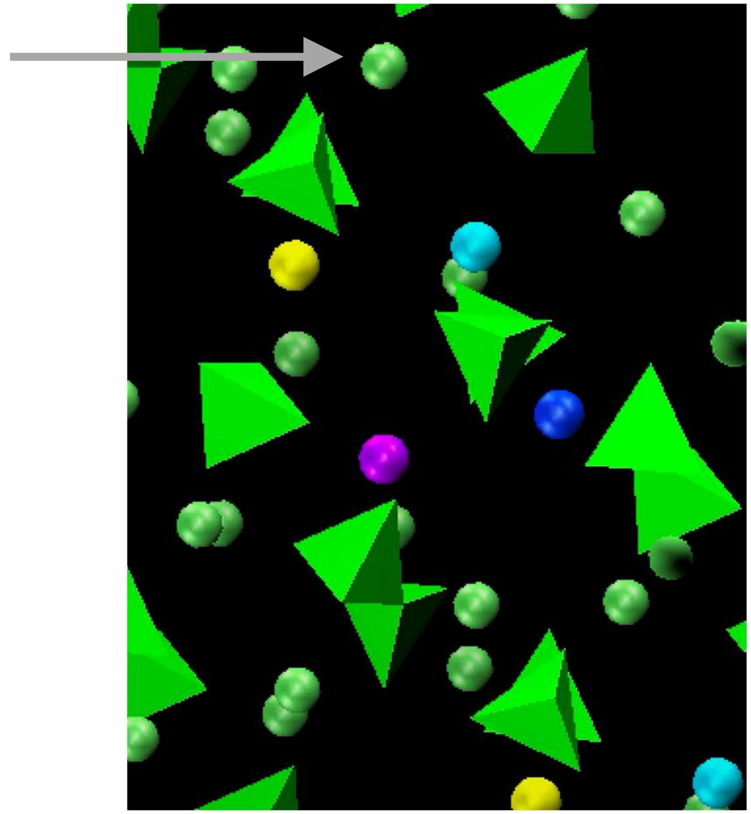

C. Wang, K. Aoyagi, P. Wisesa, and T. Mueller, Chemistry of Materials **32**, 9, 3741–3752 (2020)

Ensuring high accuracy

Moment tensor potentials can be highly accurate for local configurations similar to ones used to train them.

Sometimes a configuration unlike any in the training set is encountered.

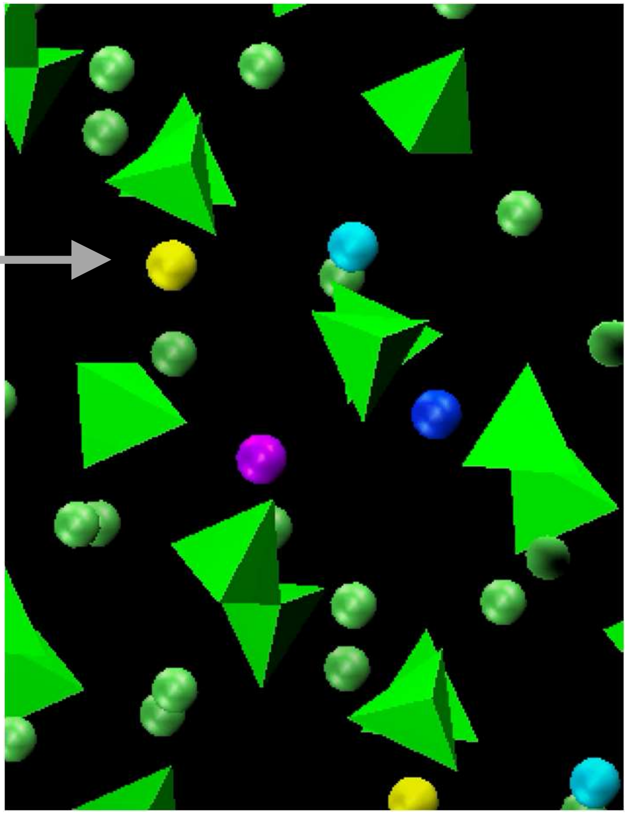

C. Wang, K. Aoyagi, P. Wisesa, and T. Mueller, Chemistry of Materials **32**, 9, 3741–3752 (2020)

Learning on the fly

JOHNS HOPKINS
WHITING SCHOOL
of ENGINEERING

Moment tensor potentials can be highly accurate for local configurations similar to ones used to train them.

When encountering a new configuration, potentials can "learn on the fly": the new configuration is automatically added to the training data and the potential is retrained to ensure accuracy.

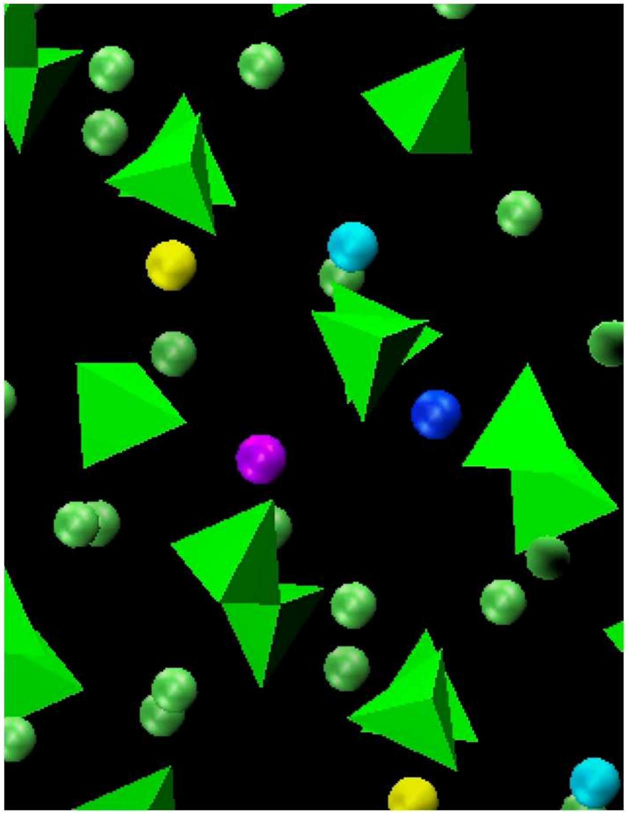

C. Wang, K. Aoyagi, P. Wisesa, and T. Mueller, Chemistry of Materials **32**, 9, 3741–3752 (2020)

Learning on the fly

Moment tensor potentials can be highly accurate for local configurations similar to ones used to train them.

When encountering a new configuration, potentials can "learn on the fly": the new configuration is automatically added to the training data and the potential is retrained to ensure accuracy.

The resulting potential generates molecular dynamics data seven orders of magnitude faster than ab-initio molecular dynamics with nearly the same accuracy.

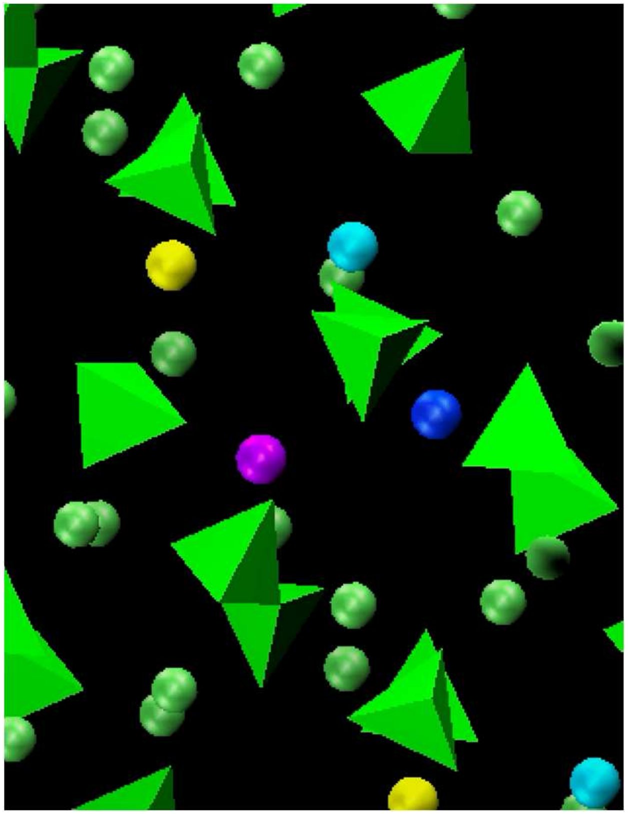

C. Wang, K. Aoyagi, P. Wisesa, and T. Mueller, Chemistry of Materials **32**, 9, 3741–3752 (2020)

Better Arrhenius plots

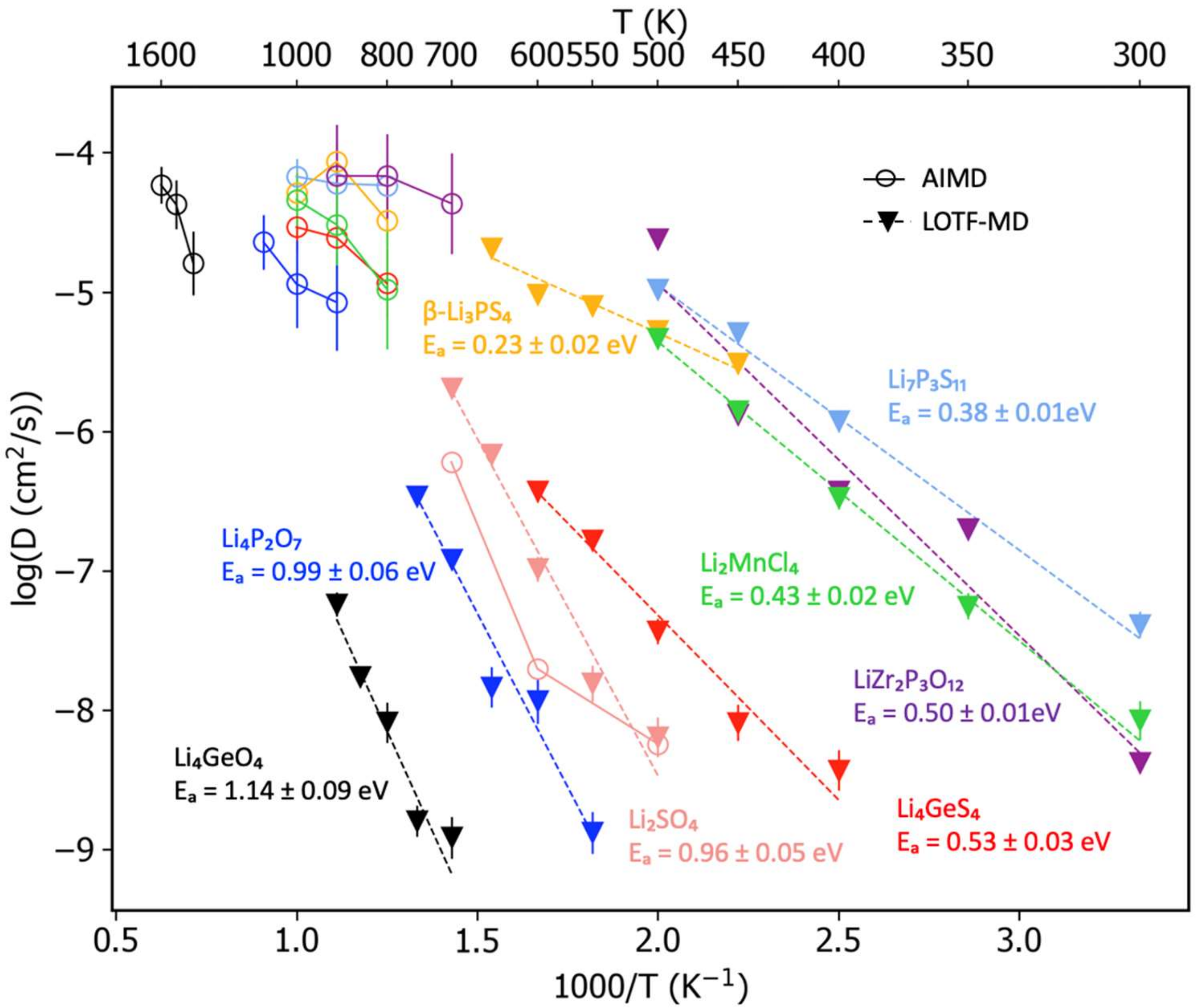

C. Wang, K. Aoyagi, P. Wisesa, and T. Mueller, Chemistry of Materials **32**, 9, 3741–3752 (2020)

Better experimental validation

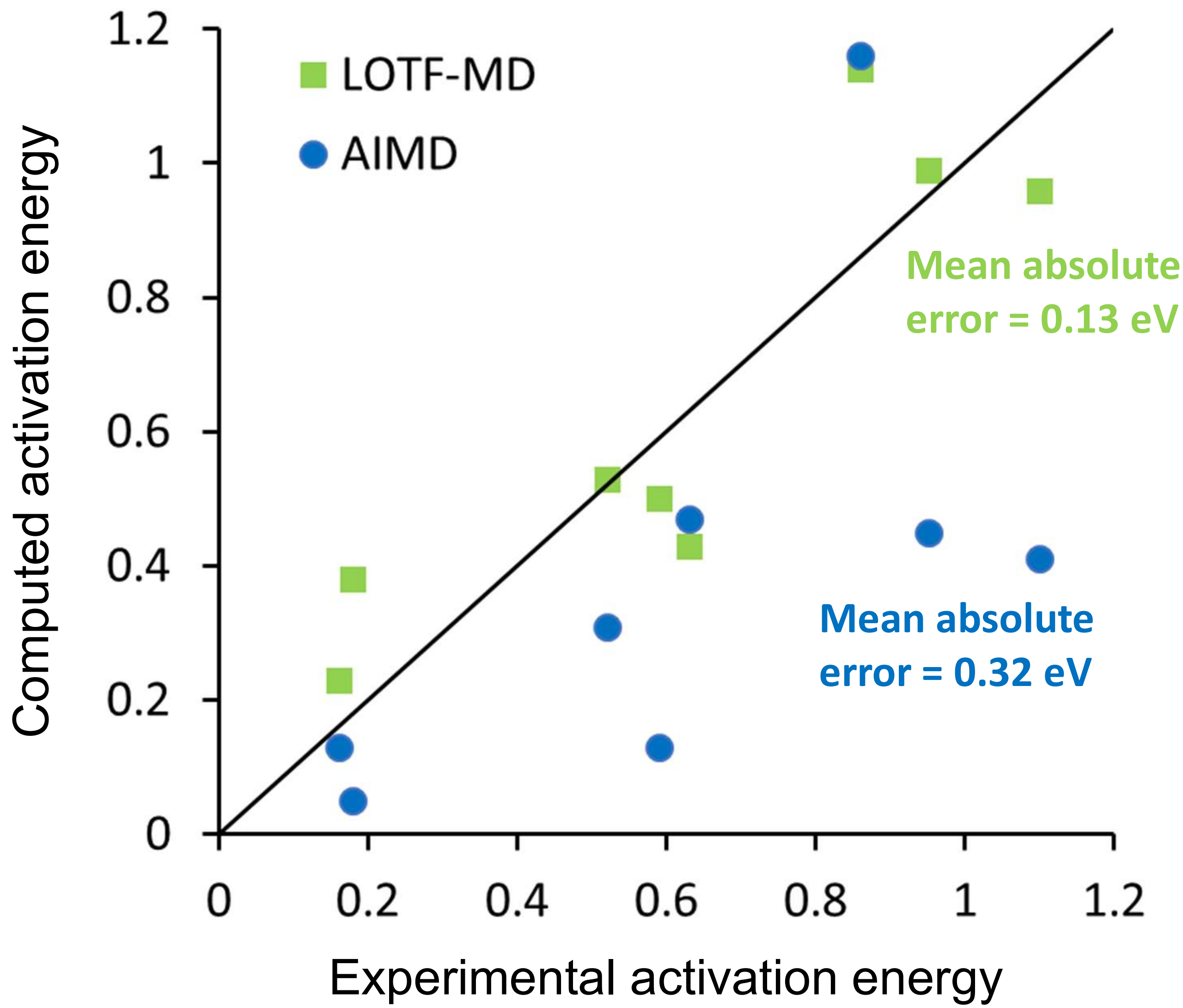

C. Wang, K. Aoyagi, P. Wisesa, and T. Mueller, Chemistry of Materials **32**, 9, 3741–3752 (2020)

New candidate coating materials

$Li_3B_7O_{12}$

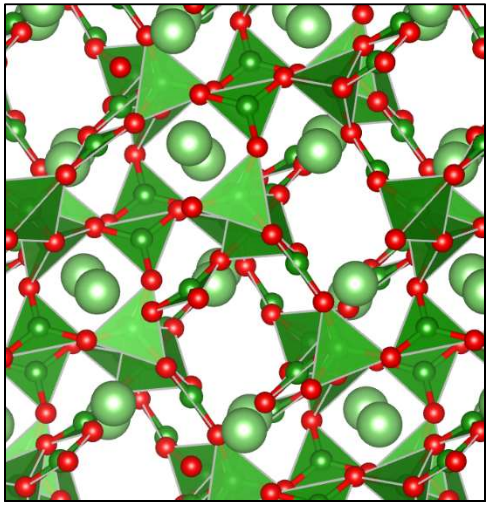

Solid-state electrolytes	Coating	Cathodes
$Li_7P_3S_{12}$ $Li_{10}GeP_2S_{12}$ $Li_{10}SnP_2S_{12}$ $Li_{10}SiP_2S_{12}$ Li_6PS_5Br Li_6PS_5Cl	$Li_3B_7O_{12}$ E_a = 0.56 eV	$LiCoO_2$ $LiFePO_4$ $LiMn_2O_4$ $Li(MnNiCo)_{1/3}O_2$ $LiMn_{1.5}Ni_{0.5}O_2$

$Li_3Sc_2(PO_4)_3$

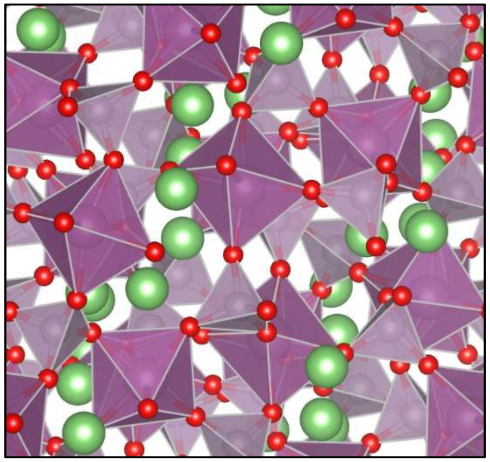

Solid-state electrolytes	Coating	Cathodes
$Li_7P_3S_{12}$	$Li_3Sc_2(PO_4)_3$ E_a = 0.64 eV	$LiFePO_4$ $Li(MnNiCo)_{1/3}O_2$

C. Wang, K. Aoyagi, P. Wisesa, and T. Mueller, Chemistry of Materials **32**, 9, 3741–3752 (2020)

Speed considerations

Moment tensor potentials are among the fastest machine-learned interatomic potential models, but they are still 1-2 orders of magnitude slower than widely-used physics-derived models like the embedded atom method.

Supervised machine learning

Supervised machine learning

1. Select a hypothesis space

Supervised machine learning

1. Select a hypothesis space

Functions that can be created by combining addition subtraction, multiplication, division, exponentiation, distance, sum over neighbors, constant values.

Supervised machine learning

1. Select a hypothesis space

Functions that can be created by combining addition subtraction, multiplication, division, exponentiation, distance, sum over neighbors, constant values.

Many physics-derived models exist in this hypothesis space: Coulomb, Lennard-Jones, harmonic potentials, embedded atom method, bond order potentials…

Supervised machine learning

1. Select a hypothesis space

Functions that can be created by combining addition subtraction, multiplication, division, exponentiation, distance, sum over neighbors, constant values.

Functions are represented as trees.

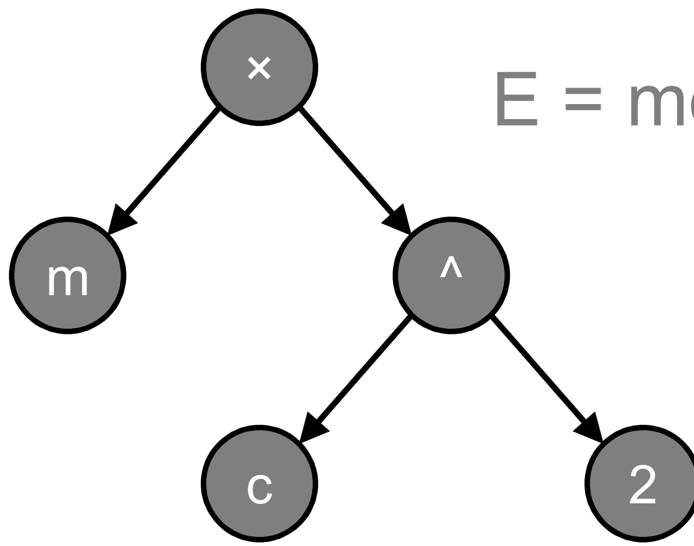

$E = mc^2$

Supervised machine learning

2. Select an objective function

Supervised machine learning

2. Select an objective function

Find candidates on convex hull with respect to

- <u>Fitness</u>
  Based on errors with respect to standardized energies, forces, and virial stresses.

Supervised machine learning

2. Select an objective function

Find candidates on convex hull with respect to

- <u>Fitness</u>

- <u>Speed</u>
  Faster models can handle larger time and length scales.

Supervised machine learning

2. Select an objective function

Find candidates on convex hull with respect to

- Fitness
- Speed
- Complexity
  Simpler models are less likely to overfit training data.

ML-IAP: Extrapolability

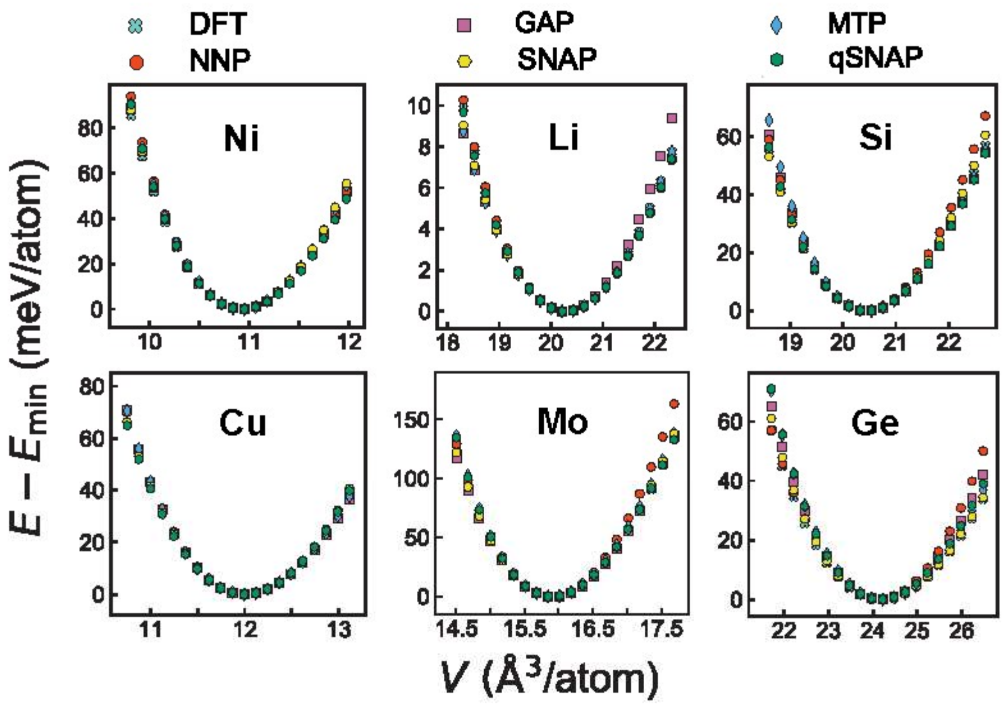

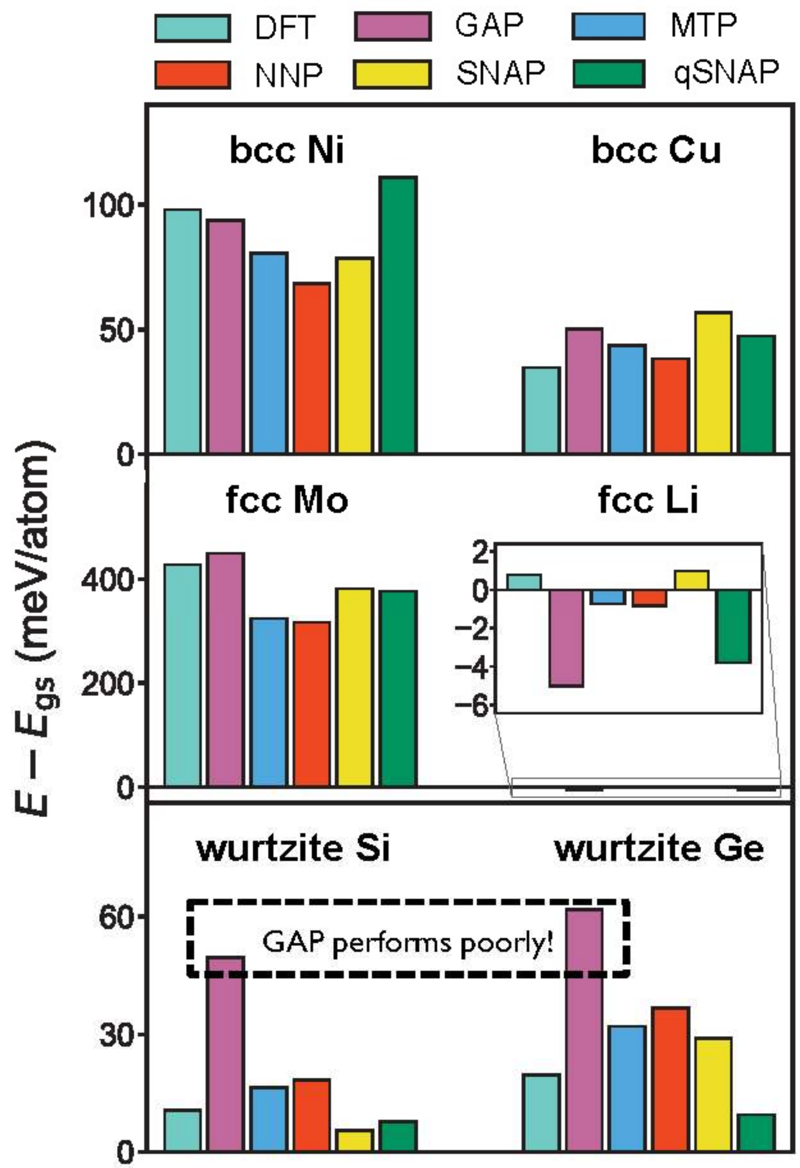

- The greater the **ML** complexity (e.g., **NNP** and **GAP**), the greater the issues with extrapolation.
- Linear **SNAP** performs surprisingly well on **EOS** and polymorph energy differences.

Zuo et al. A Performance and Cost Assessment of Machine Learning Interatomic Potentials. arXiv:1906.08888 2019.

Supervised machine learning

3. Search the hypothesis space

Supervised machine learning

3. Search the hypothesis space

This problem is known as “symbolic regression”.

Supervised machine learning

3. Search the hypothesis space

This problem is known as “symbolic regression”.

We use an approach called “genetic programming”, in which functions evolve using an evolutionary algorithm.

Evolutionary step: Crossover

$$\sum(1-r)+14 \qquad (r+11)*\sum(3+r)$$

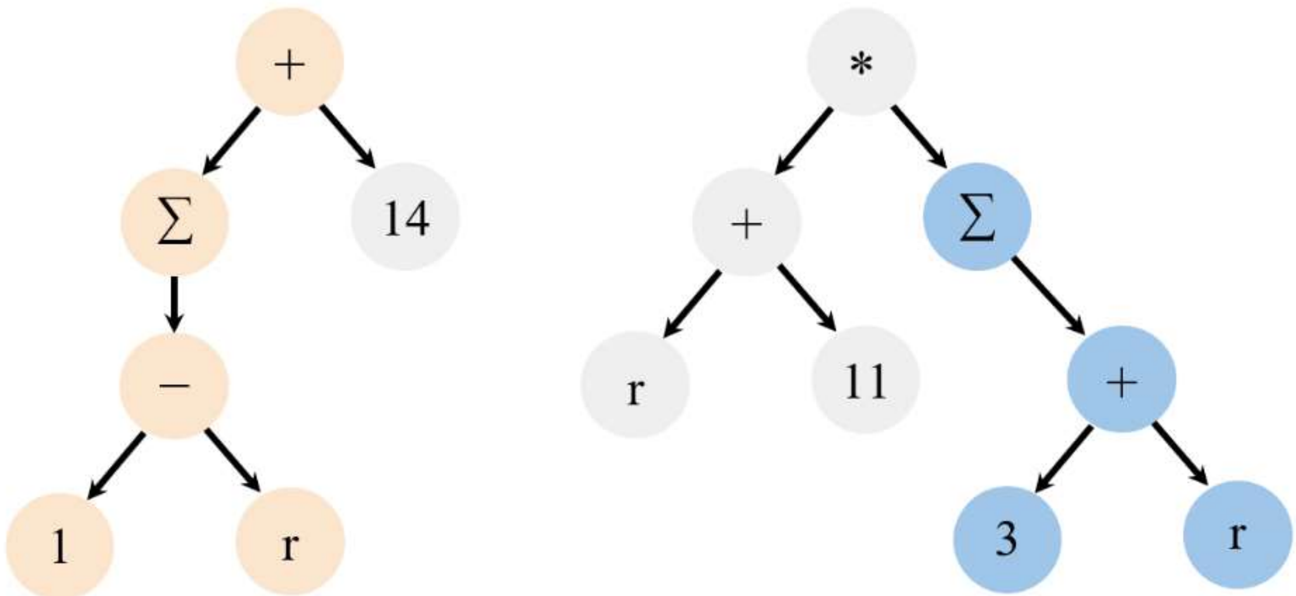

Evolutionary step: Crossover

$$\sum(1-r)+ \qquad\qquad \sum(3+r)$$

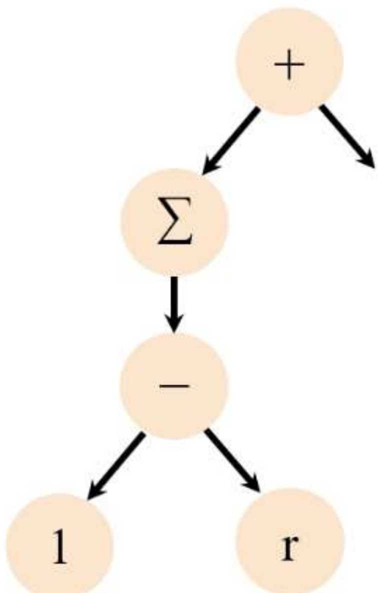

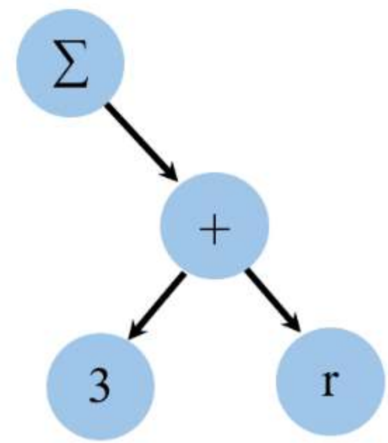

Evolutionary step: Crossover

$$\sum(1-r)+\sum(3+r)$$

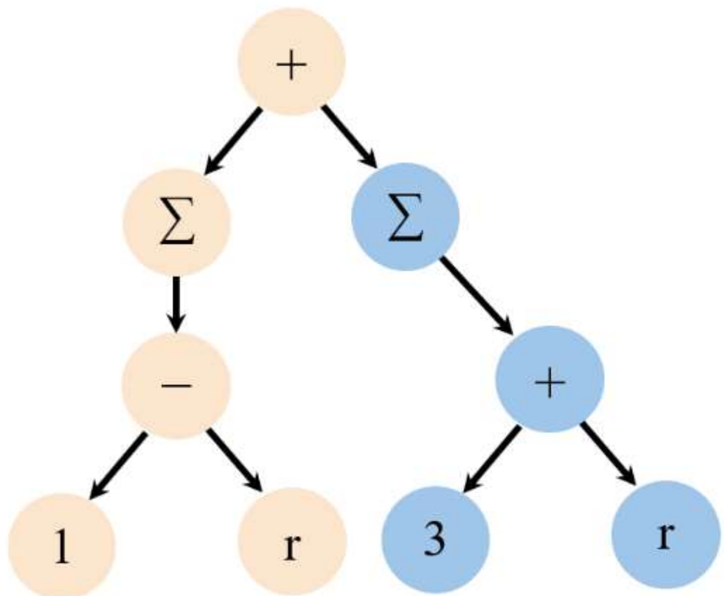

Evolutionary step: Mutation

$$\sum(1-r)$$

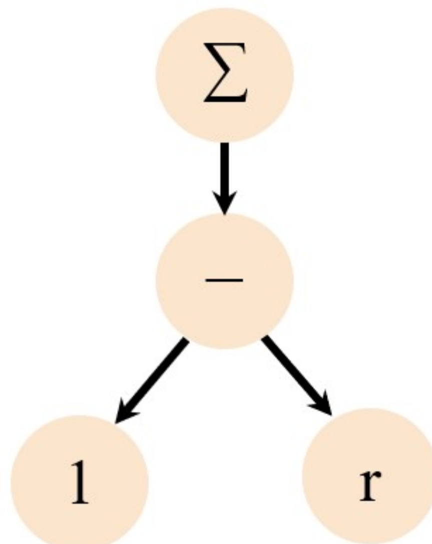

Evolutionary step: Mutation

$$\sum(1+r)$$

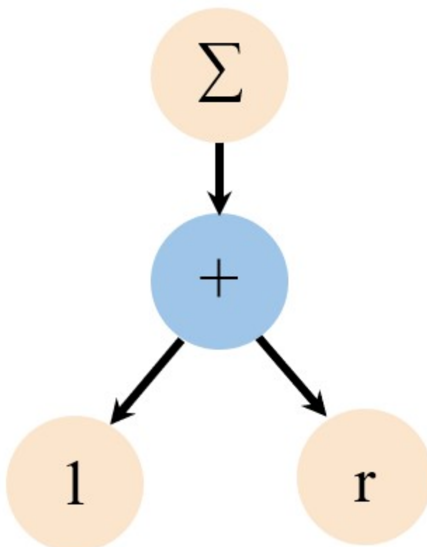

Evolutionary step: Mutation

$$\sum (1 - r)$$

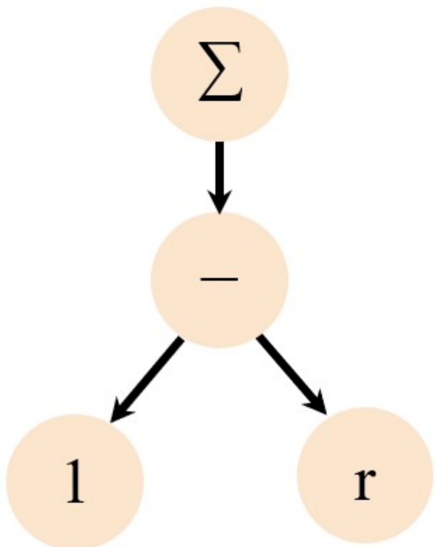

Evolutionary step: Mutation

$$\sum (r - 1)$$

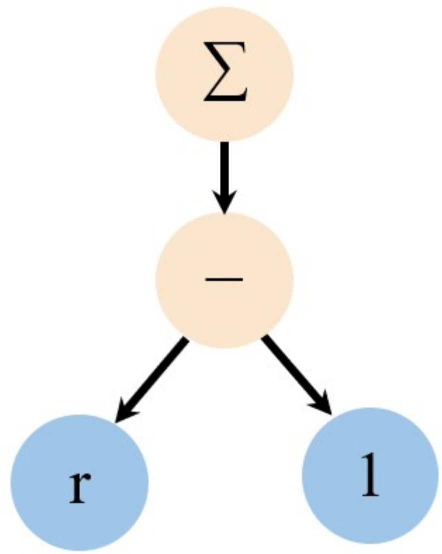

Evolutionary step: Mutation

$$\sum (r - 1)$$

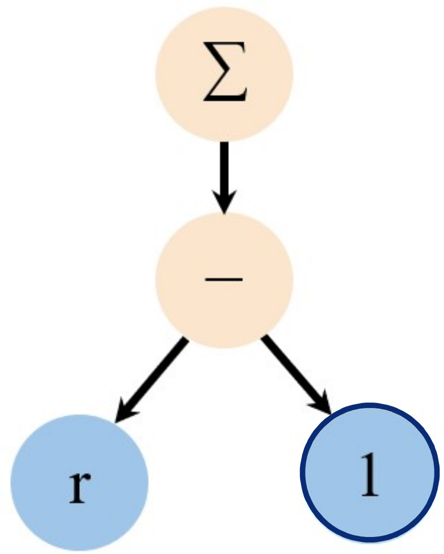

We use conjugate gradient and CMA-ES to optimize the parameters.

Regenerating the embedded atom method

Potential model used to generate training data
$$V_{SC} = \sum_i \left(\sum_j \frac{644.52}{r^9} - \left(\sum_j \frac{527.62}{r^6} \right)^{0.5} \right)$$

(Sutton and Chen, Philosophical Magazine Letters, 1990)

Regenerating the embedded atom method

Potential model used to generate training data

$$V_{SC} = \sum_i \left(\sum_j \frac{644.52}{r^9} - \left(\sum_j \frac{527.62}{r^6} \right)^{0.5} \right)$$

(Sutton and Chen, Philosophical Magazine Letters, 1990)

Potential model found by genetic programming

$$V = \sum_i \left(-0.73 - 2.53 \left(\left(-0.66(384.39) \sum_j r^{-9.00} \right) + \left(0.25 / \left(20.63 \sum_j r^{-6.00} \right) \right)^{-0.50} \right) \right)$$

A. Hernandez, A. Balasubramanian, F. Yuan, S. A. M. Mason and T. Mueller
npj Computational Materials **5**, 112 (2019)

Regenerating the embedded atom method

Potential model used to generate training data

$$V_{SC} = \sum_i \left(\sum_j \frac{644.52}{r^9} - \left(\sum_j \frac{527.62}{r^6} \right)^{0.5} \right)$$

(Sutton and Chen, Philosophical Magazine Letters, 1990)

Potential model found by genetic programming (simplified)

$$V = \sum_i \left(-0.73 + \sum_j \frac{644.55}{r^{9.00}} - \left(\sum_j \frac{527.32}{r^{6.00}} \right)^{0.50} \right)$$

A. Hernandez, A. Balasubramanian, F. Yuan, S. A. M. Mason and T. Mueller
npj Computational Materials **5**, 112 (2019)

New models for copper from DFT data

GP1
$$\sum\left(r^{10.21-5.47r}-0.21^{r}\right)f(r)+0.97\left(\sum 0.33^{r} f(r)\right)^{-1}$$

GP2
$$V=7.33\sum r^{3.98-3.94r} f(r)+\left(27.32-\sum\left(11.13+0.03r^{11.74-2.93r}\right)f(r)\right)\left(\sum f(r)\right)^{-1}$$

$f(r)$ is a tapering function.

A. Hernandez, A. Balasubramanian, F. Yuan, S. A. M. Mason and T. Mueller
npj Computational Materials **5**, 112 (2019)

Pareto frontier for elastic constants

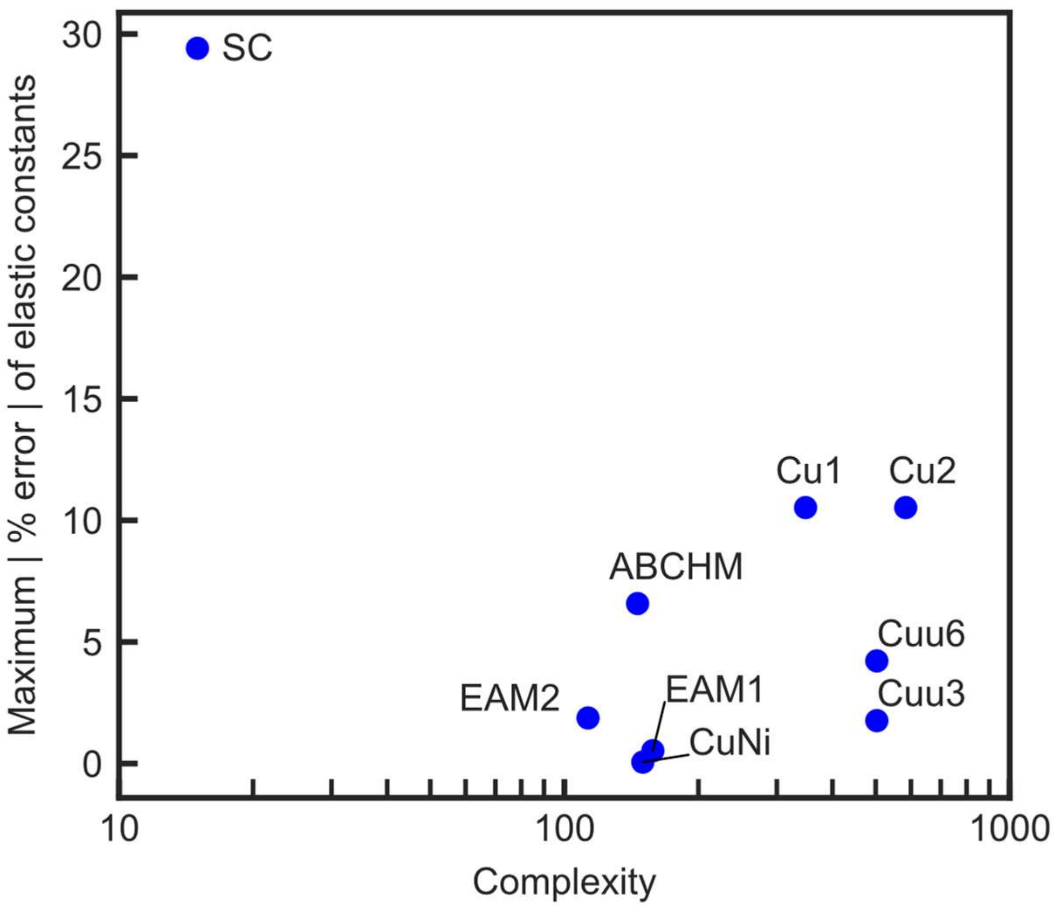

SC: (Sutton and Chen 1990), ABCHM and Cu1: (Mendelev, Kramer et al. 2008), EAM1 and 2: (Mishin, Mehl et al. 2001), Cu2: (Mendelev and King 2013), Adams: (Adams, Foiles et al. 1989). Cuu3: (Becker et al., Current Opinion in Solid State and Materials Science, 2013), CuNi: (Onat and Durukanoglu, JPCM, 2013)

Pareto frontier for elastic constants

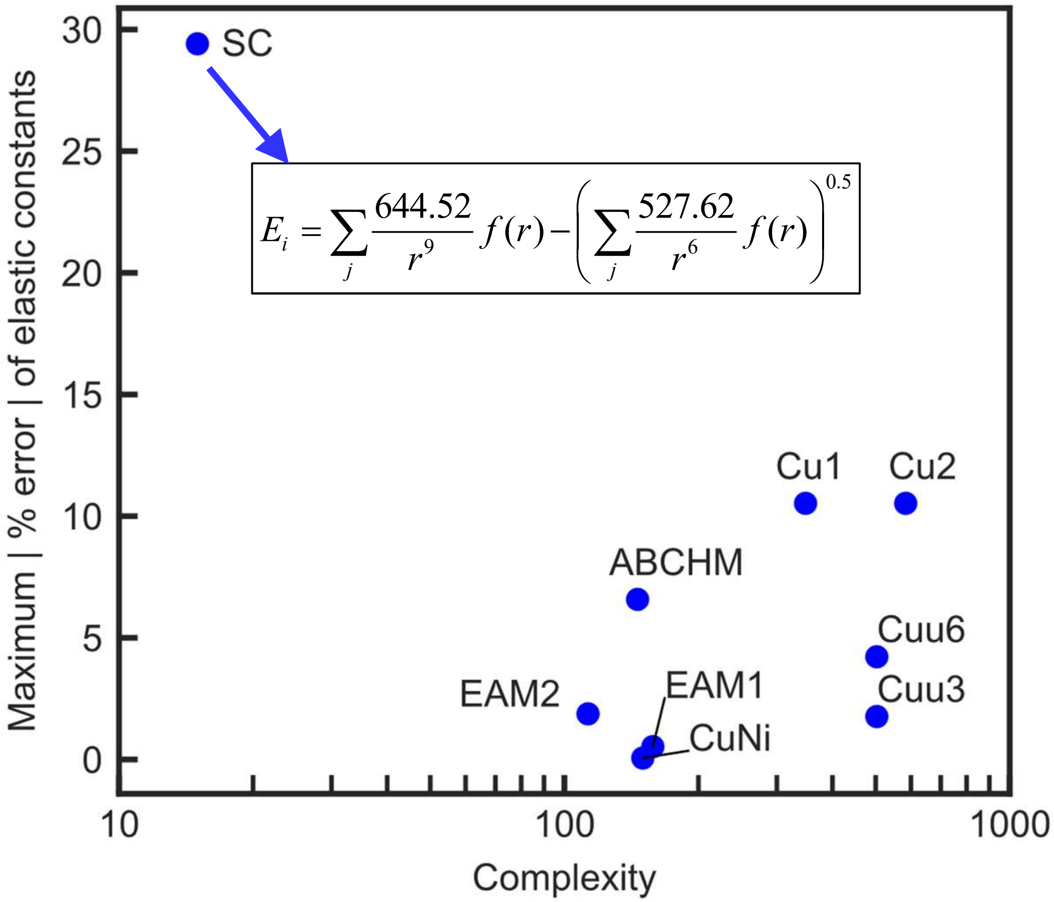

SC: (Sutton and Chen 1990), ABCHM and Cu1: (Mendelev, Kramer et al. 2008), EAM1 and 2: (Mishin, Mehl et al. 2001), Cu2: (Mendelev and King 2013), Adams: (Adams, Foiles et al. 1989). Cuu3: (Becker et al., Current Opinion in Solid State and Materials Science, 2013), CuNi: (Onat and Durukanoglu, JPCM, 2013)

Pareto frontier for elastic constants

$$E_i = \frac{1}{2}\sum_j \left(D_M \left[1 - e^{-\alpha_M (r - R_M)} \right]^2 - D_M \right) f(r) + F(\bar{\rho}_i)$$

$$\bar{\rho}_i = \sum_j \tanh(20 r^2) \left\{ r^6 \left(e^{-\beta r} + 2^9 e^{-2\beta r} \right) + \frac{\sigma^{(1)}}{\mu^{(1)}} e^{-\frac{1}{2}\left[\mu^{(1)}(r - R_B)\right]^2} - 0.1\sigma^{(1)} e^{-\frac{1}{2}\left[\mu^{(1)}(r - (R_B + 0.5))\right]^2} \right\} f(r)$$

$$\sum_i F(\bar{\rho}_i) = -E_{sub}(1 + a^*) e^{-a^*} - \frac{1}{2}\sum_i \sum_j \left(D_M \left[1 - e^{-\alpha_M (r - R_M)} \right]^2 - D_M \right) f(r)$$

$$a^* = (a / a_0 - 1) / (E_{sub} / 9B\Omega)^{1/2}$$

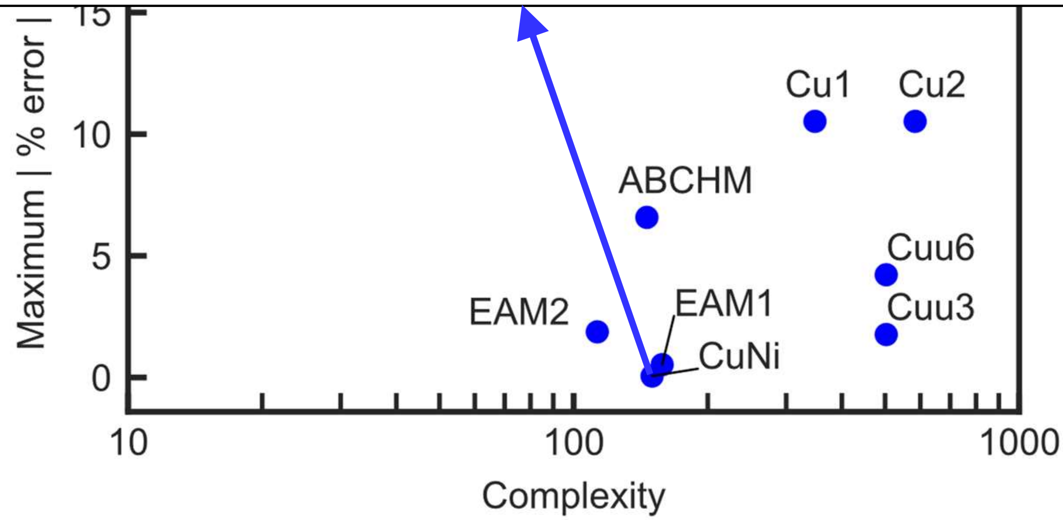

SC: (Sutton and Chen 1990), ABCHM and Cu1: (Mendelev, Kramer et al. 2008), EAM1 and 2: (Mishin, Mehl et al. 2001), Cu2: (Mendelev and King 2013), Adams: (Adams, Foiles et al. 1989). Cuu3: (Becker et al., Current Opinion in Solid State and Materials Science, 2013), CuNi: (Onat and Durukanoglu, JPCM, 2013)

Pareto frontier for elastic constants

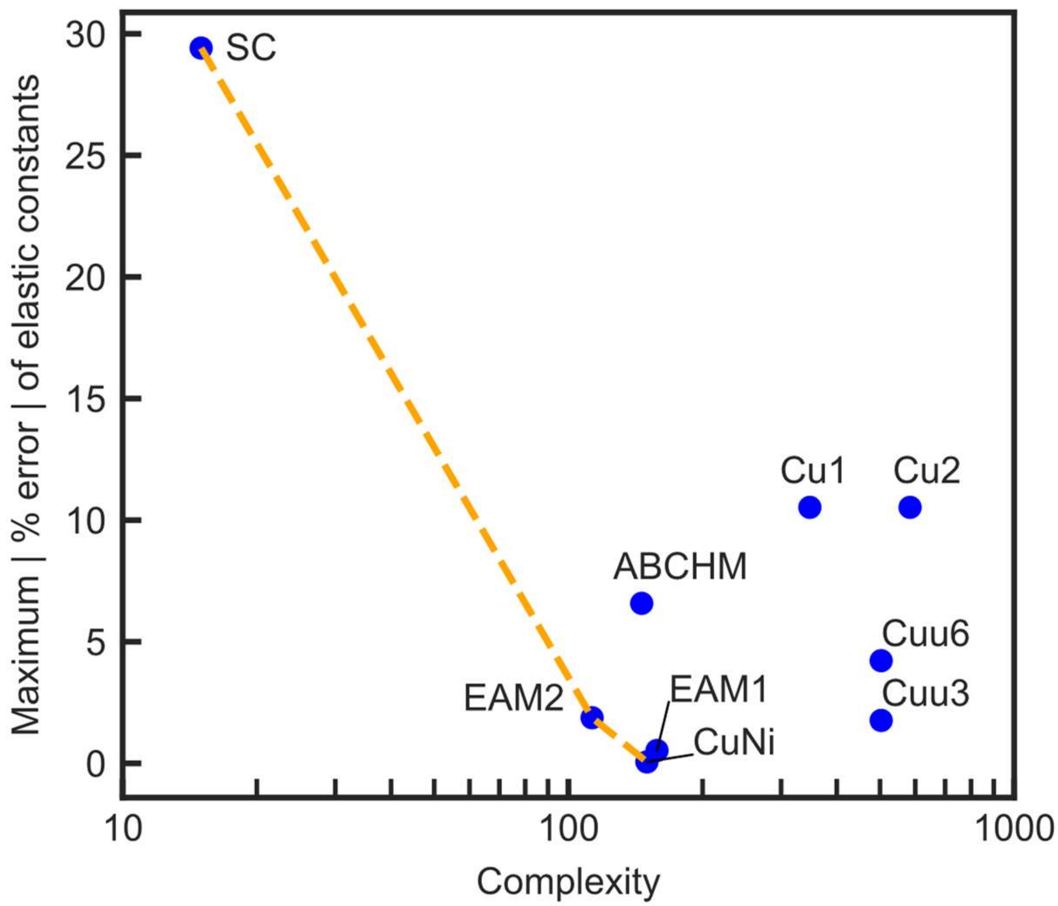

SC: (Sutton and Chen 1990), ABCHM and Cu1: (Mendelev, Kramer et al. 2008), EAM1 and 2: (Mishin, Mehl et al. 2001), Cu2: (Mendelev and King 2013), Adams: (Adams, Foiles et al. 1989). Cuu3: (Becker et al., Current Opinion in Solid State and Materials Science, 2013), CuNi: (Onat and Durukanoglu, JPCM, 2013)

Pareto frontier for elastic constants

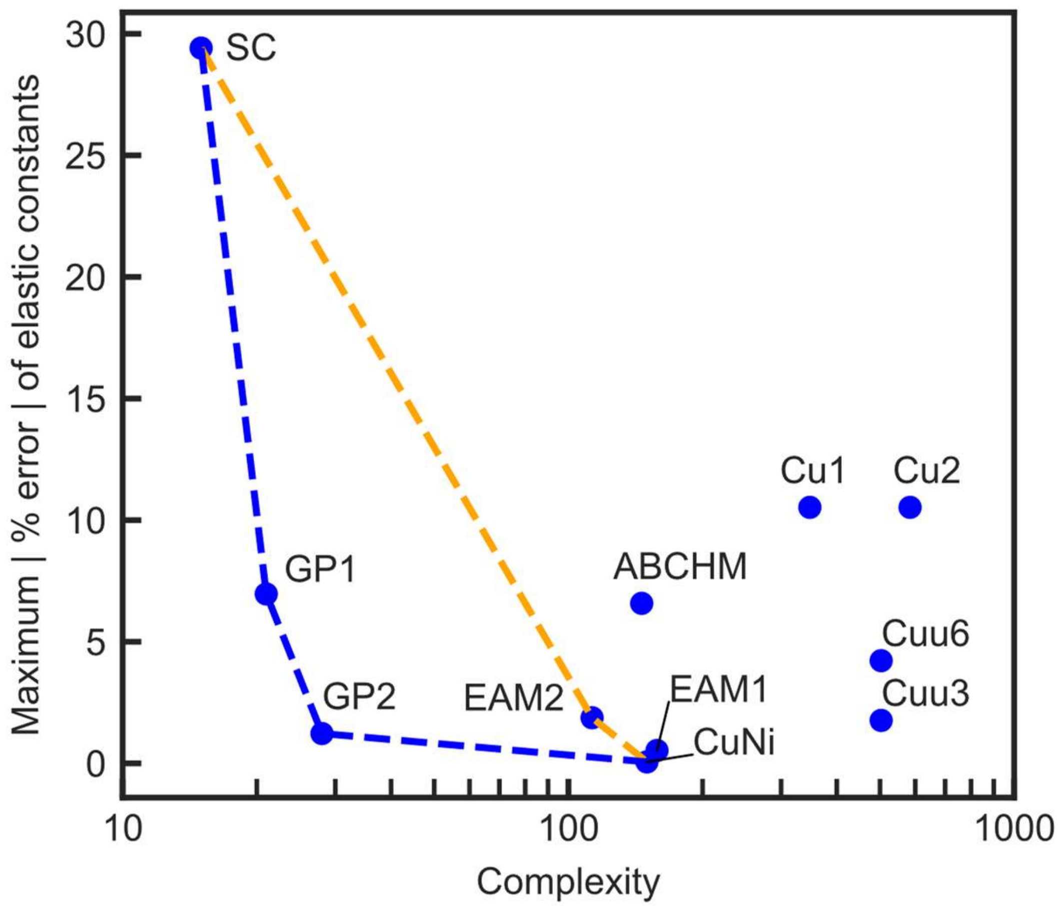

SC: (Sutton and Chen 1990), ABCHM and Cu1: (Mendelev, Kramer et al. 2008), EAM1 and 2: (Mishin, Mehl et al. 2001), Cu2: (Mendelev and King 2013), Adams: (Adams, Foiles et al. 1989). Cuu3: (Becker et al., Current Opinion in Solid State and Materials Science, 2013), CuNi: (Onat and Durukanoglu, JPCM, 2013)

Training and validation errors are similar

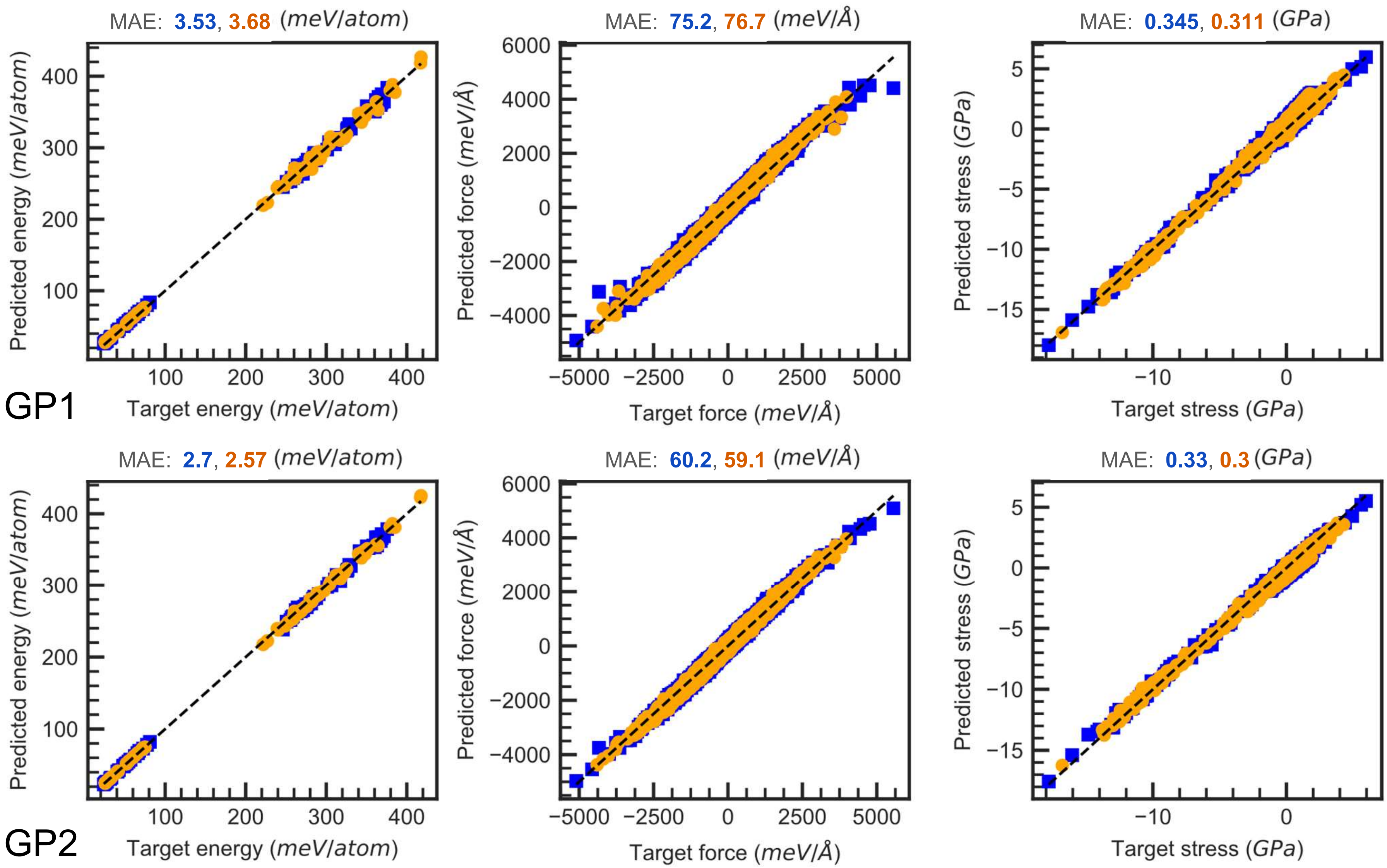

Blue is validation, orange is training. MAE: validation, training

GP1 and GP2 are transferable

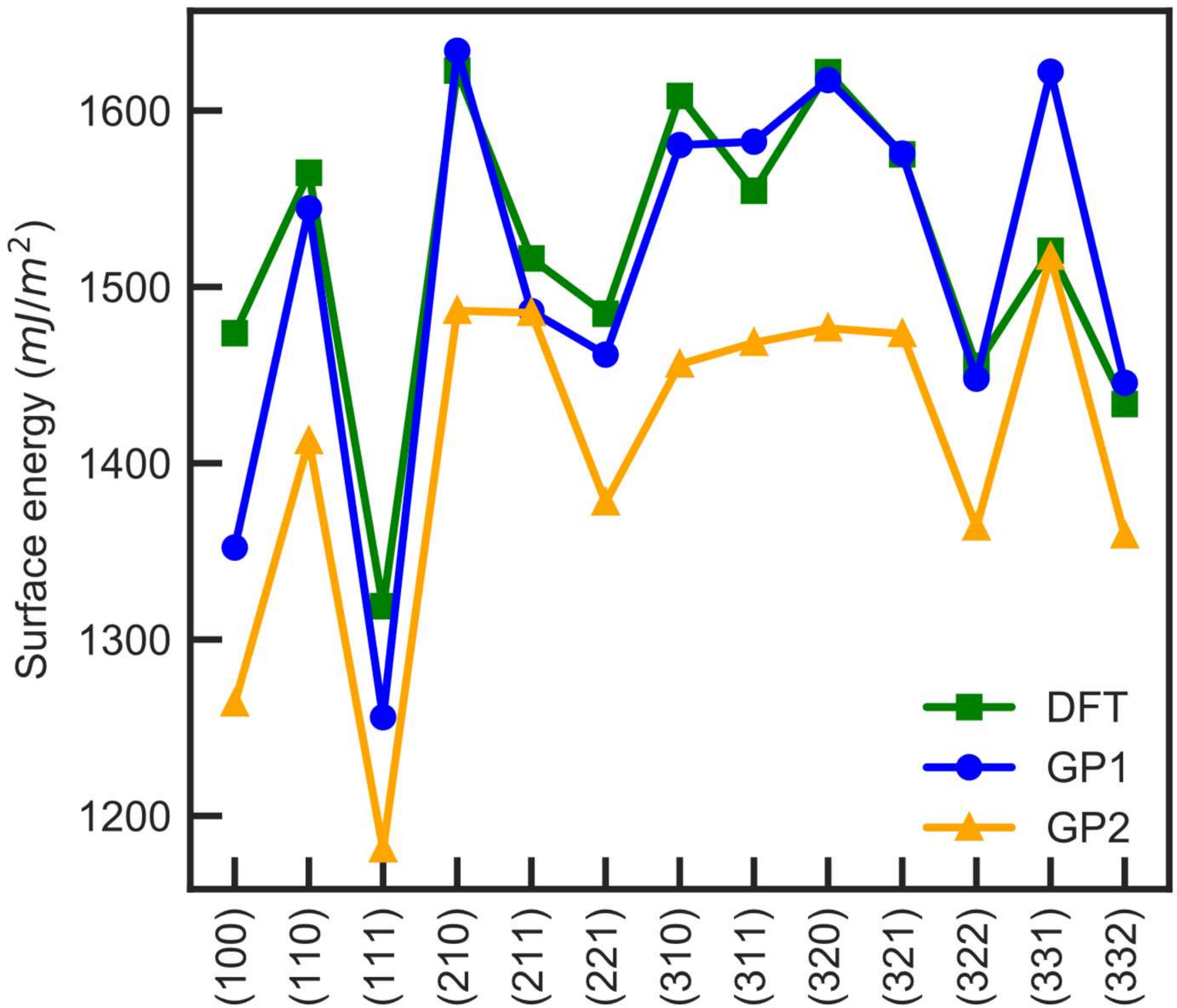

A. Hernandez, A. Balasubramanian, F. Yuan, S. A. M. Mason and T. Mueller
npj Computational Materials **5**, 112 (2019)

GP1 and GP2 are transferable

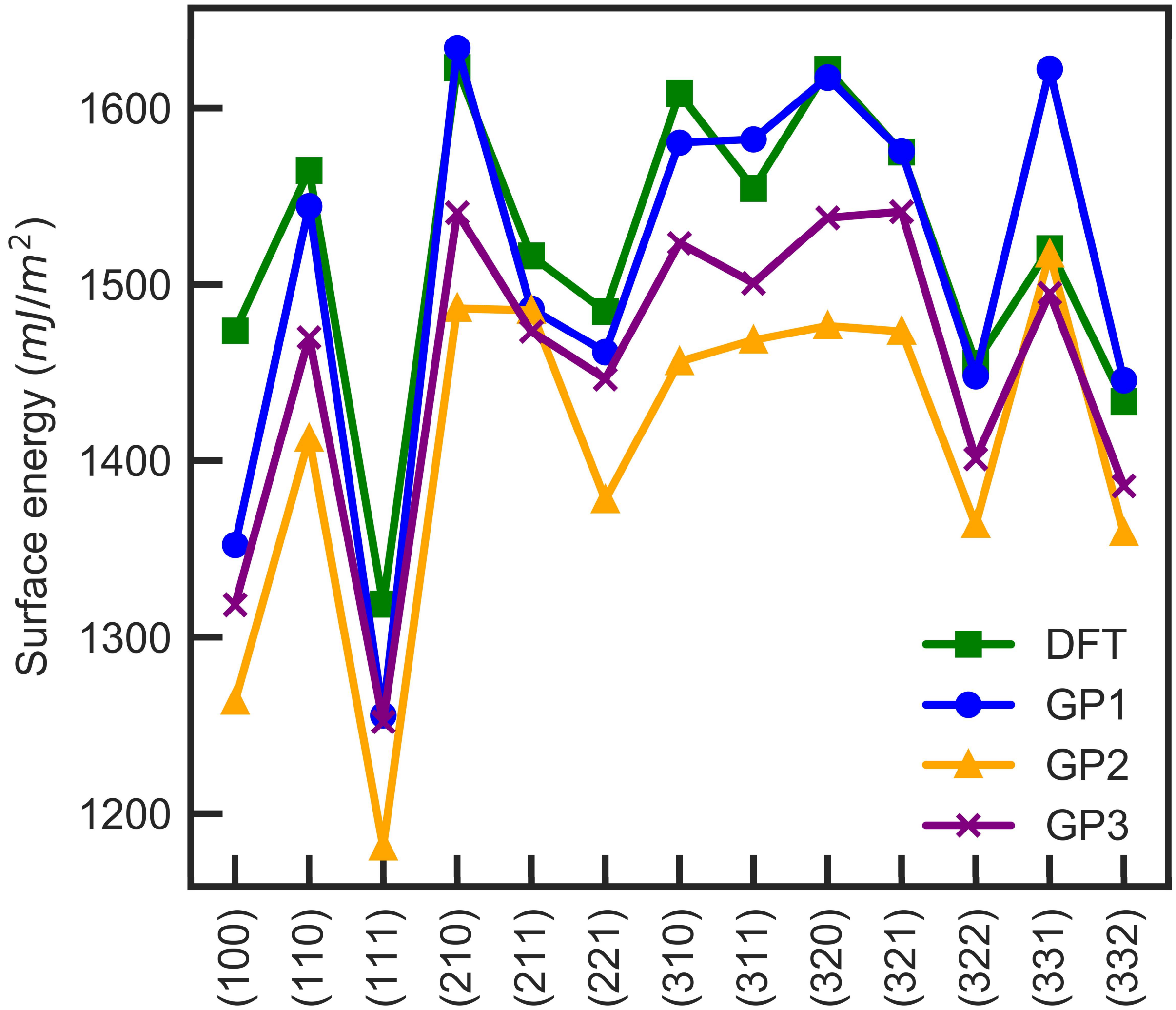

A. Hernandez, A. Balasubramanian, F. Yuan, S. A. M. Mason and T. Mueller
npj Computational Materials **5**, 112 (2019)

Low prediction errors

JOHNS HOPKINS
WHITING SCHOOL of ENGINEERING

	GP3	ABCHM	CuNi	EAM1	EAM2	Cuu3	Cuu6
bcc lattice constant |Å|	0.2	2.4	0.9				
bcc-fcc formation energy |meV / atom|	12	11	13		2		
hcp-fcc formation energy |meV / atom|	2		4		6		
vacancy migration energy |meV|	49		20			40	20
dumbbell formation energy |meV|	15	250					
phonon frequencies at X |% error|	2.1				4.4		
phonon frequencies at L and K |% error|	2.5		2.6	4.1	5.5		
intrinsic stacking fault energy |mJ / m^2|	6		0		9		

Lowest testing error (green)

Testing error (yellow)

A. Hernandez, A. Balasubramanian, F. Yuan, S. A. M. Mason and T. Mueller
npj Computational Materials **5**, 112 (2019)

Very fast execution

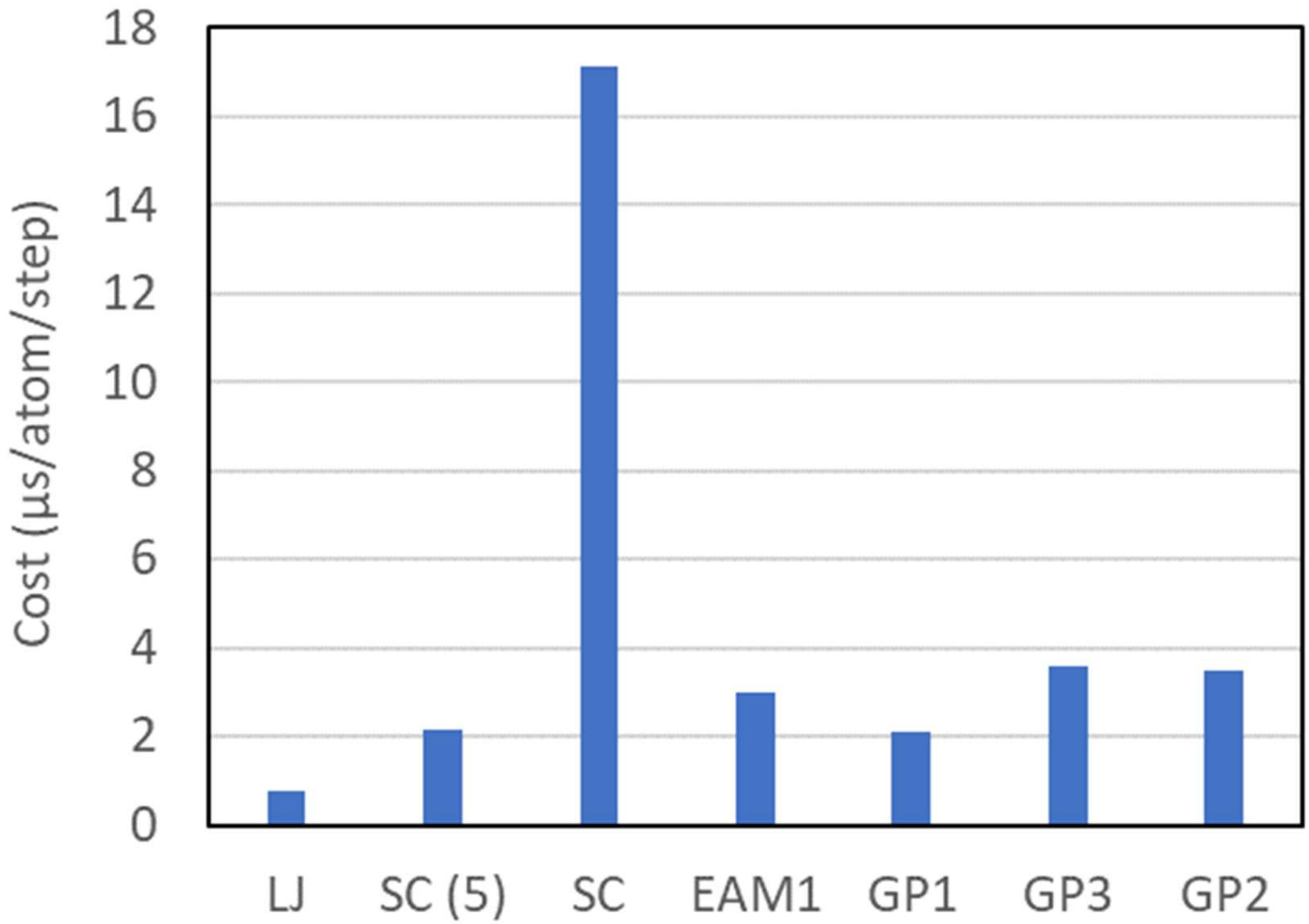

A. Hernandez, A. Balasubramanian, F. Yuan, S. A. M. Mason and T. Mueller
npj Computational Materials **5**, 112 (2019)

Additional resources

Open source code for potential generation using genetic programming

https://gitlab.com/muellergroup/poet

Tools for automatically generating efficient *k*-point grids

http://muellergroup.jhu.edu/K-Points.html
https://arxiv.org/abs/1907.13610
https://gitlab.com/muellergroup/k-pointGridGenerator
https://gitlab.com/muellergroup/kplib